

Ecological Vulnerability Assessment and Cause Analysis of the Farming–Pastoral Zone in Northern China—Taking Yulin City as an Example



Yanmei Zhong, Jianguo Cheng, Lingkui Meng, and Wen Zhang

Abstract The farming–pastoral zone in China is located in the monsoonal region. It has large fluctuations in precipitation and land use. It is one of the most obvious areas of ecological vulnerability. Taking Yulin City of Shanxi Province as an example, this paper builds an indicator system and then uses principal component analysis (PCA) and analytic hierarchy process (AHP) to filter indicators and determine weights. Finally, this paper establishes an ecological vulnerability index (EVI) model. Through the classification of EVI, the spatial distribution map of ecological vulnerability in Yulin City is obtained. The results show that the ecological vulnerability in Yulin City tends to decrease from north to south. Among counties, Fugu, Shenmu, Yuyang and Dingbian are extremely fragile, and the main causes of ecological vulnerability are economics, landscape diversity, annual precipitation and vegetation coverage.

Keywords Remote sensing · Ecological vulnerability · Principal component analysis · AHP · Cause analysis

1 Introduction

When ecosystem is intervened by outside, it will make sensitive reactions and self-recovery reactions, and this is ecological vulnerability [1]. China's farming–pastoral zone is located in the monsoon climate zone of Southeast Asia, and with large precipitation fluctuations, has characteristic of fragile ecology. Yulin City is an area where ecology is particularly fragile. The ecological environment research of Yulin and the whole farming–pastoral zone has attracted extensive attention from scholars. However, the main method for ecological assessment of Yulin is single-factor evaluation method [2–6]. And a few methods for ecological vulnerability evaluation still have

Y. Zhong · L. Meng · W. Zhang (✉)

School of Remote Sensing and Information Engineering, Wuhan University, Wuhan 430079, China

e-mail: wen_zhang@whu.edu.cn

J. Cheng

Information Center of Ministry of Water Resources, Beijing 100053, China

© Springer Nature Singapore Pte Ltd. 2020

L. Wang et al. (eds.), *Proceedings of the 6th China High Resolution Earth Observation Conference (CHREOC 2019)*, Lecture Notes in Electrical Engineering 657,

https://doi.org/10.1007/978-981-15-3947-3_11

problems of large correlation between indicators and strong subjectivity of weight determination [7–9]. These years, remote sensing is used in ecological research, and it makes data acquisition simpler and data types more abundant [10–12]. This paper uses remote sensing, meteorological and statistical yearbook data, principal component analysis (PCA) and analytic hierarchy process (AHP) to obtain ecological vulnerability index and analyzes the overall status, spatial distribution and causes of ecological vulnerability of Yulin.

2 Study Area

Yulin is located in the northernmost part of Shanxi Province, between N 36°57′ – N 39°35′ and E 107°28′–E 111°15′. It has typical semiarid and arid climate, and the average annual precipitation is close to 400 mm. There are three landforms: windblown grass beach, loess hilly and gully, and beam-shaped low hills. The mineral resource is diverse and rich in total. It is an important energy export city in China. Special climate, topography, soil texture and high-intensity human activities make it a typical ecologically fragile area in the northern farming–pastoral zone.

3 Methods and Data

3.1 Construction of Ecological Vulnerability Indicator System

This paper constructs an evaluation indicator system from three aspects: ecological sensitivity, ecological restoration and ecological stress [13, 14]. Taking into account the availability of data, 13 indicators were chosen to constitute the indicator system. The indicator system is shown in Fig. 1.

3.2 Evaluation Indicator Selection and Weight Determination

3.2.1 Standardization of Primary Selection Indicators

We standardize the primary selection indicators to make them be unified to 0–1, so that the values are closer to 1 indicating that the ecology is more fragile [4]. Eight indicators of temperature, elevation, slope, aspect, soil erodibility factor, soil erosion intensity, GDP density and population density are positively correlated with ecological vulnerability; landscape diversity index, vegetation coverage, precipitation, relative humidity and GPP are negatively correlated with ecological vulnerability.

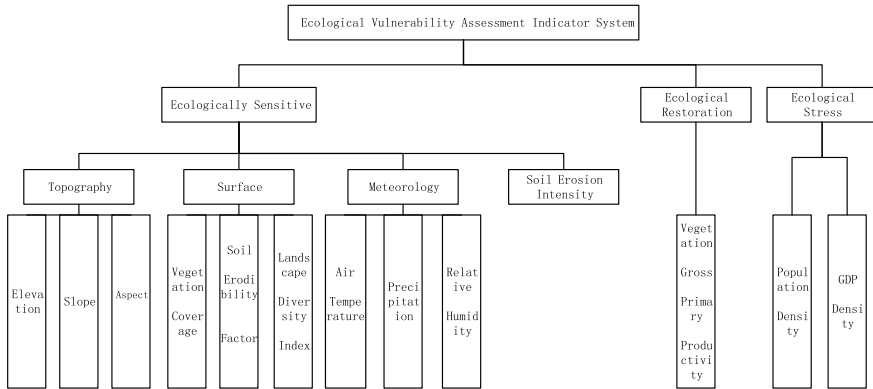


Fig. 1 Ecological vulnerability assessment indicator system

The standardized formulas are shown in Eqs. 1 and 2, respectively.

$$\text{positively correlated: } P^{*i} = (P_i - P_{\min}) / (P_{\max} - P_{\min}) \tag{1}$$

$$\text{negatively correlated: } P^{*i} = 1 - (P_i - P_{\min}) / (P_{\max} - P_{\min}) \tag{2}$$

P^{*i} represents the value after the normalization of the i th evaluation indicator, P^i represents the value before the i th evaluation indicator is normalized, P_{\max} represents the maximum value of the i th evaluation indicator, and P_{\min} represents the minimum value of the i th evaluation indicator [4].

3.2.2 Selection of Evaluation Indicators

We use the PCA to analyze 13 standardized primary evaluation indicators [15–19]. Table 1 shows the results of sorting the principal components according to the contribution value. The cumulative contribution rate of the first five is 86.81%, which is more than 85%, indicating that the first five principal components can cover most information of the primary selection indicators, so the first five principal components are selected as evaluation indicators. Table 2 shows eigenvectors corresponding to each principal component.

3.2.3 Determination of Indicator Weights

We use AHP to determine indicator weights. The assignment principle of the pairwise comparison matrix is shown in Table 3. The larger the value, the greater the influence of the i th element on the previous indicator layer compared to the j th element.

Table 1 Principal component contribution rate and cumulative contribution rate

Principal component	Eigenvalues	Contribution rate (%)	Cumulative contribution rate (%)
1	0.10317	32.7911	32.7911
2	0.08283	26.3266	59.1177
3	0.03872	12.3056	71.4233
4	0.03104	9.8670	81.2902
5	0.01737	5.5220	86.8123
6	0.01226	3.8962	90.7085
7	0.00934	2.9697	93.6782
8	0.00720	2.2894	95.9676
9	0.00390	1.2381	97.2057
10	0.00341	1.0833	98.2890
11	0.00252	0.8021	99.0910
12	0.00156	0.4959	99.5869
13	0.00130	0.4131	100.00

Table 2 Eigenvectors corresponding to each principal component

Eigenvector	Principal component				
	1	2	3	4	5
α_1	0.64236	-0.27545	0.32387	-0.03409	0.04721
α_2	-0.11891	-0.25524	-0.16227	0.06069	0.08317
α_3	-0.00889	0.01013	0.01042	-0.01733	0.09875
α_4	-0.01328	0.09345	0.16424	0.97881	0.06298
α_5	0.02509	0.27287	0.09066	-0.02346	-0.06305
α_6	0.08523	0.12261	-0.12268	-0.00493	0.16803
α_7	0.44726	0.28017	0.46675	-0.07925	-0.11404
α_8	0.16351	0.28050	-0.05602	-0.00666	0.08573
α_9	-0.32953	-0.19795	0.55427	-0.11678	0.70066
α_{10}	-0.32737	0.49174	0.36467	-0.09927	-0.25902
α_{11}	-0.07814	-0.00431	0.15554	-0.05549	-0.03140
α_{12}	-0.28965	0.15145	0.14463	-0.04015	-0.15021
α_{13}	0.18040	0.54730	-0.33484	-0.04125	0.58566

α_1 – α_{13} : GDP density, population density, soil erodibility factor, aspect, DEM, GPP, landscape diversity index, relative humidity, soil erodibility factor, annual precipitation, slope, annual average temperature, vegetation coverage

Table 3 Assignment of pairwise comparison matrix

Scaling	Meaning
1	Element <i>i</i> and element <i>j</i> have the same importance to the previous-level factor
3	Element <i>i</i> is slightly more important than element <i>j</i>
5	Element <i>i</i> is more important than element <i>j</i>
7	Element <i>i</i> is much more important than element <i>j</i>
9	Element <i>i</i> is extremely more important than element <i>j</i>
2, 4, 6, 8	Indicates the intermediate value of the above adjacent judgment
Reciprocal	$A_{ji} = 1/A_{ij}$

This paper constructs a pairwise comparison matrix based on the contribution rates of the first five principal components. Equation 3 is proposed to calculate relative importance scale, A_{ij} represents the relative importance scale of elements *i* and *j*, and α_i and α_j represent the contribution rates of elements *i* and *j*. *A* is the pairwise comparison matrix constructed. After calculation, the weights of the evaluation indicators are: 0.5350, 0.2868, 0.0853, 0.0555, 0.0374.

$$A_{ij} = \frac{(\alpha_i - \alpha_j)}{3.4086} + 1, (i < j) \tag{3}$$

$$A = \begin{vmatrix} 1 & 3 & 7 & 8 & 9 \\ 1/3 & 1 & 5 & 6 & 7 \\ 1/7 & 1/5 & 1 & 2 & 3 \\ 1/8 & 1/6 & 1/2 & 1 & 2 \\ 1/9 & 1/7 & 1/3 & 1/2 & 1 \end{vmatrix}$$

3.3 Evaluation Model

The five evaluation indicators are graded by the natural discontinuity grading method shown in Table 4. The higher the level, the higher the ecological vulnerability.

In Eq. 4, EVI represents the ecological vulnerability index; w_i represents the weight of the *i*th evaluation indicator; f_i represents the level of the *i*th evaluation indicator [4].

$$EVI = \sum_{i=1}^n w_i f_i \tag{4}$$

Table 4 Indicators' grading results

Grade	Principal component				
	1	2	3	4	5
1	0–0.47	0.09–0.46	0–0.71	0–0.36	0–0.52
2	0.47–0.79	0.46–0.74	0.71–0.93	0.36–0.56	0.52–0.71
3	0.79–1.18	0.74–1.03	0.93–1.16	0.56–0.76	0.71–0.88
4	1.18–1.58	1.03–1.42	0.16–1.40	0.76–0.97	0.88–1.08
5	1.58–1.94	1.42–2.03	1.40–1.82	0.97–1.33	1.08–1.62

3.4 Data Sources and Preprocessing

The soil erosion intensity is calculated according to RUSLE model (modified general soil loss model) based on the above data [20–22]. Thirteen indicators are unified into 1 km resolution, UTM_Zone_49N (Table 5).

Table 5 Data sources

Data type	Data resource	Indicator
Soil	HWSD	Soil erodibility factor
Vegetation type	MCD12Q1	Landscape diversity index
Statistical data	Shanxi provincial bureau of statistics	Population and GDP density
Topographic	SRTM	Elevation, slope and aspect
GPP	MOD17A2	Annual average GPP
Vegetation coverage	MOD13A2	Vegetation coverage index
Meteorological	China meteorological data network	Temperature, humidity, precipitation

Table 6 Division of ecological vulnerability levels in Yulin

Vulnerability level	EVI value	Area ($\times 10^3$ km ²)	Proportion of total area (%)
Micro	<1.9	9.17	21.8
Mild	1.9–2.7	4.26	10.1
Moderate	2.7–3.2	9.59	22.8
Severe	3.2–3.6	10.83	25.7
Extreme	>3.6	8.26	19.6

4 Results and Analysis

4.1 Overall State of Ecological Vulnerability

The EVI is classified as shown in Table 6. Yulin has the largest area with severe vulnerability, accounting for 25.7% of the city's area. Moderate and above vulnerability account for nearly 70% of the city's area, and only 20% of the city's area is micro-vulnerability.

4.2 Spatial Distribution of Ecological Vulnerability

The distribution of ecological vulnerability levels is shown in Fig. 2. The proportion of vulnerability levels in various districts and counties is shown in Fig. 3. The ecological vulnerability level of Yulin is characterized by high north and low south. Fugu, Shenmu, Yuyang and Dingbian are most fragile. These four counties have 20–45% extremely vulnerable areas. Especially in Shenmu, extremely vulnerable areas account for 45% of the county's area.

4.3 Analysis of the Causes of Ecological Vulnerability

Figure 4 depicts the standardized evaluation indicators of various districts and counties in Yulin. The closer the evaluation indicator is to 1, the greater the vulnerability of the county. The main causes of ecological vulnerability in Dingbian are single landscape, low vegetation coverage and low precipitation. The reason for the ecological vulnerability of Fugu and Shenmu is human production activities and single landscape types. These two counties develop coal industry vigorously, and this leads to a decline in landscape diversity and increase in ecological vulnerability. The main reason for the ecological vulnerability of Yuyang is the landscape type is not rich enough and coupled with the pressure of human activities on the environment, and vegetation coverage is low. The main reason for the ecological fragility in Jingbian

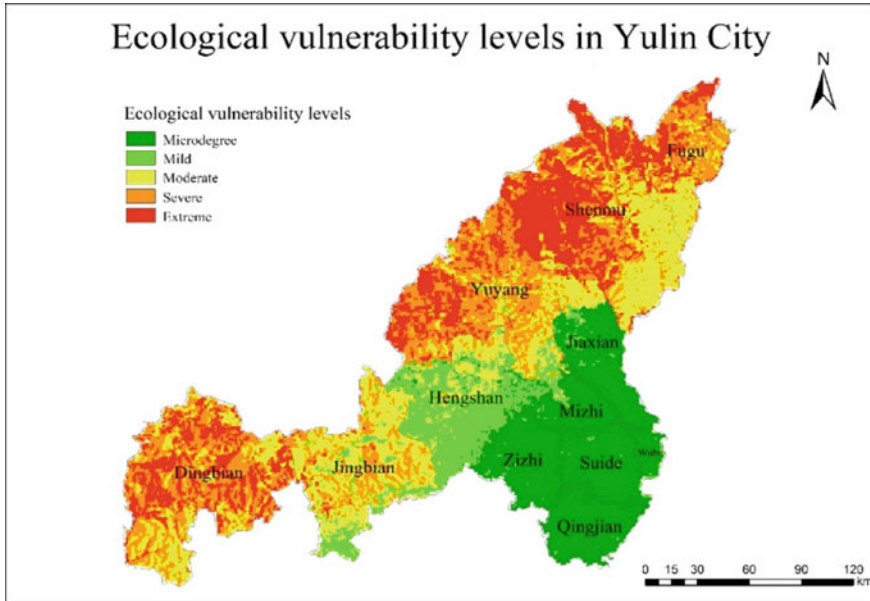
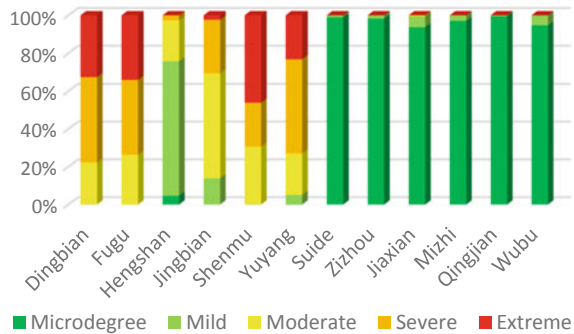


Fig. 2 Spatial distribution of ecological vulnerability levels in Yulin City

Fig. 3 Statistics on ecological vulnerability levels of various districts and counties in Yulin City



is that the landscape type is not rich and the precipitation is small. The 5/6 population in Jingbian is agricultural population, and less precipitation in arid areas will restrict the growth of crops and reduce the stability of the agricultural and livestock ecosystem. Vegetation coverage and aspect are the main reasons for the ecological fragility of Hengshan. There is a large area of half-sunny slope in Hengshan, and water evaporation on sunny slope is fast, which is not conducive to vegetation growth. One of the most obvious features of the six southern counties is the large *K* value and high vegetation coverage, and the vegetation has a tightening effect on the soil thus decreasing EVI.

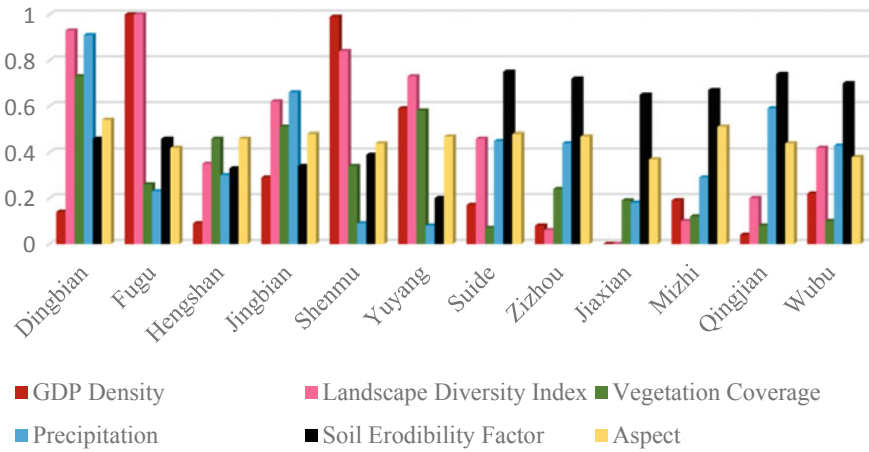


Fig. 4 Evaluation indicators after standardization in various districts and counties of Yulin City

5 Summary

This paper processes remote sensing, and meteorological and socioeconomic data, and uses PCA and AHP to calculate EVI. The main research results were as follows:

1. The method of combining PCA and AHP is used to construct the EVI model, which reduces the correlation between indicators and improves the objectivity of weight determination.
2. Obtain the distribution map of vulnerability level. It is found that the ecological of six northern counties is more fragile than six southern counties. The extremely fragile areas are Fugu, Shenmu, Yuyang and Dingbian.
3. The main causes for the ecological vulnerability of the farming–pastoral zone in Yulin were economics, landscape diversity, annual precipitation and vegetation coverage.

Acknowledgements Fund projects National Key Research and Development Program of China (2017YFC0405806).

References

1. Zhengjia L, Xingxiu Y, Lei L, Mei H (2011) Vulnerability assessment of eco-environment in Yimeng mountainous area of Shandong Province based on SRP conceptual mode. *Chin J Appl Ecol* 8:2084–2090
2. Qiufang S, Peihao P, Jie H, Liu Z, Xiaofei S, Huaiyong S (2016) Monitoring eco-environmental vulnerability in Anning River Basin in the upper reaches of the Yangtze River using remote sensing techniques. *Remote Sens Land Resour* 28(2):175–181

3. Furong (2008) Remote sensing monitoring of ecological environment in the typical region of fragile ecological restoration in the farming-pastoral ecotone—Taking Zhenglan banner as an example. Inner Mongolia Normal University
4. Pan L, Deyong H, Wenji Z (2010) The monitoring of changes of land vegetation covers by remote sensing in farming-pastoral mixed zones of North Chiana—A case study in Guyuan County, Hebei Provinc. *Remote Sens Land Resour* 2:113–117
5. Jiangbo G, Wenjuan H, Dongsheng Z, Shaohong. W (2016) Comprehensive assessment of natural ecosystem vulnerability in Tibetan Plateau based on satellite-derived datasets. *Sci Geogr Sin* 4:580–587
6. Jingli L (2009) Quantitative evaluation of Gansu Wen County soil erosion based on RUSLE model. Lanzhou University
7. Jing Z (2016) Based on RS and GIS the Erguna Wetlands ecological vulnerability assessment. Southwest Jiaotong University
8. Wei D, Xingzhong Y, Rong S, Yuewei Z (2016) Eco-vulnerability Assessment based on remote sensing in the argo-pastoral ecotone of North China. *Environ Sci Technol* 39(11):174–181
9. Shao H, Liu M, Shao Q, Sun X, Wu J (2014) Research on eco-environmental vulnerability evaluation of the Anning River Basin in the Upper Reaches of the Yangtze River. *Environ Earth Sci* 72(5):1555–1568
10. Shuang X, Runping S, Xiaoyue Y (2012) A comparative study of different vegetation indices for estimating vegetation coverage based on the dimidiate pixel model. *Remote Sens Land Resour* 4:95–100
11. Scanlon TM, Albertson JD, Caylor KK, Williams CA (2002) Determining land surface fractional cover from NDVI and rainfall time series for a savanna ecosystem. *Remote Sens Environ* 82(2):376–388
12. Carlson TN, Ripley DA (1997) On the relation between NDVI, fractional vegetation cover, and leaf area index. *Remote Sens Environ* 62(3):241–252
13. Tingting X (2016) Assessment of soil erosion in karst area Based on RUSLE model—A case study in the Southwest of Songzi. Huazhong University of Science and Technology
14. Yonghua L, Qiang F, Xue W et al (2015) Spatial and temporal differentiation of ecological vulnerability under the frequency of natural hazard based on SRP model: A case study in Chaoyang county. *Sci Geogr Sin* 35(11):1452–1459
15. Jian S, Jun C (2012) Principal component analysis and its application (A). *Light Ind Technol*. 9:12–13
16. Vaughan RA (1990) A review of: “Introduction to Remote Sensing”. In: Campbell JB (ed) The Guilford Press, Guilford, 1987. p 551. Price£ 34.95. *Remote Sen* 11(10):1932
17. Jensen JR Lulla K (2007) Introductory digital image processing: a remote sensing perspective. Science Press
18. Lillesand T, Kiefer RW, Chipman J (2000) Remote sensing and image interpretation, 6th edn. Remote sensing and image interpretation. Wiley, pp 3035
19. Elkington MD (1987) A review of: “Remote Sensing Digital Image Analysis: An Introduction”. In: Richards JA (ed) Springer, Berlin, Heidelberg. New York, 1986, p 281. Price DM (1987) 138. *Int J Remote Sen* 8(7):1075–1075
20. Bin W, Jinbai H, Xinglong G (2015) Grid soil moisture constants estimation based on HWSO over basin. *Hydrology* 35(2):8–11
21. Bin W, Xingchen D, Jinbai H et al (2017) Grid runoff parameters estimation and adjustment of GSAC model based on HWSO. *Trans Chin Soc Agric Mach* 48(9):250–256
22. Nachtergaele FO, Velthuisen H, Verelst L et al (2012) Harmonized world soil database (version 1.2)